LETTER

Computational study of electron paramagnetic resonance spectra for Li and Ga vacancies in $LiGaO_2$

Computational Study of Electron Paramagnetic Resonance Spectra for Li and Ga Vacancies in $LiGaO_2$

Dmitry Skachkov* and Walter R. L. Lambrecht
Department of Physics, Case Western Reserve University, 10900 Euclid Avenue, Cleveland, Ohio 44106-7079, USA

Klichchupong Dabsamut and Adisak Boonchun
Department of Physics, Faculty of Science, Kasetsart University, Bangkok 10900 Thailand

A first-principles computational study of the Electron Paramagnetic Resonance (EPR) parameters of Li and Ga vacancies in $LiGaO_2$ is presented. In the EPR active charge states of the neutral lithium vacancy ($V_{\rm Li}^0$) and doubly negative ionized gallium vacancy ($V_{\rm Ga}^{2-}$), the spin is localized on one of the O neighbors of the vacancy. We compare the calculated EPR parameters for spin density localized on different O neighbors. Good agreement with experiment is obtained for both the g-tensor values and principal axes orientations and the superfhyperfine interaction parameters supporting the prior experimental identification of which O the spin is localized on. The g-tensor orientations are found to be close to the bond rather than the crystalline axes. The high energy of formation of $V_{\rm Ga}$ compared to $V_{\rm Li}$ also explains why $V_{\rm Ga}$ were only observed after high energy irradiation while $V_{\rm Li}$ were found in as grown samples. On the other hand, the transition levels and Fermi level position explain why $V_{\rm Li}$ required ionization from the -1 to 0 charge state to become active while $V_{\rm Ga}$ were already found in the $q = -2$ EPR active state.

$LiGaO_2$ is an ultra-wide-band-gap material with a wurtzite-like crystal structure[1,2] and experimental band gap of ∼5.3–5.7 eV at room temperature.[3–6] It can be grown in bulk form by the Czochralsky method[1] and has been suggested as a useful substrate for GaN but can also be grown by epitaxial method on ZnO and vice versa. Mixed ZnO-$LiGaO_2$ alloys have also been reported.[7,8] In fact, this material can be viewed as a I-III-VI_2 analog of the II-VI material ZnO by substituting the II-element Zn by a group I (Li) and a group III (Ga) in an ordered fashion on the wurtzite lattice. It has been considered for piezoelectric properties[9–11] in the past and is for the most part considered an insulator. However, Boonchun and Lambrecht[12] suggested it might be worthwhile considering as a semiconductor electronic material and showed in particular that it could possibly be n-type doped by Ge. In view of the recent interest in β-Ga_2O_3 as ultra-wide semiconductor for power electronics, which is also n-type by doping with Si, Sn or Ge, this makes $LiGaO_2$ worth revisiting, in particular from the point of view of defects and doping.

Recently, Electron Paramagnetic Resonance (EPR) experiments on irradiated samples of $LiGaO_2$ were reported by Lenyk *et al.*[13] and reported EPR signals for both the $V_{\rm Ga}$ and $V_{\rm Li}$. Here we present a computational study of the EPR parameters of these defects and in particular compare the calculated g-tensors and superhyperfine (SHF) interactions with both Ga and Li neighbors of the O on which the spin is localized for different possible localization sites of the spin. We will show that this confirms the experimentally deduced models for the spin-localization.

The g-tensor is calculated using the Gauge Including Projector Augmented Wave (GIPAW) method.[14–17] This is a Density Functional Perturbation Theory (DFPT) method to calculate the linear magnetic response of a periodic system onto an external magnetic field. It is implemented in the code QE-GIPAW,[18] which is integrated within the Quantum Espresso package.[19] At present the QE-GIPAW code is not yet capable of dealing with orbital dependent density functionals such as DFT+U[20–22] or hybrid functionals.[23,24] The latter are required to ensure a strong localization of the spin-density on a single O. The on-site Coulomb interaction term in the potential for orbital i, $V_i = U(\frac{1}{2} - n_i)$ shifts occupied orbital energies down by $U/2$ and empty ones up by $U/2$, thus helping to localize the hole state. We thus use DFT with on-site Coulomb corrections U on O-p orbitals with the Perdew-Burke-Ernzerhof (PBE) generalized gradient approximation (GGA) to relax the structure and also calculate the SHF interactions at this GGA+U level but calculate the g-tensor using wavefunctions at the PBE-GGA level while keeping the structure fixed. This procedure was found to be adequate in prior work on EPR parameters in β-Ga_2O_3.[25,26] The GGA+U structures were in good agreement with a previous study of the same defects[27] using the Heyd-Scuseria-Ernzerhof (HSE) hybrid functional.

We focus on the EPR active states $V_{\rm Ga}^{2-}$ and $V_{\rm Li}^0$ which both correspond to a $S = 1/2$ single unpaired electron state. We find that in the DFT+U approach with a value of $U = 4$ eV on O-p orbitals, the spin-density becomes well localized on a single O p-orbital but depending on the initial displacements given to the O, we can get it to localize on different O neighbors. Keeping this relaxed structure, the spin then stays localized on the single O even when recalculating it in GGA. We need to distinguish the following O-sites. First in the crystal structure, the O_I sits on top of Li and the O_{II} sits on top of Ga in the **c** direction. Secondly, we call an O *apical* if it sits right above the vacancy (in the **c**-direction) and *basal* if it lies in the **ab**-plane below it. The basal plane O can

TABLE I. Calculated g-tensor for Li and Ga vacancies using the GIPAW approach. In the calculated results, the g-tensor is given in terms of three principal values followed by the θ (polar) and ϕ (azimuthal) angles in degrees measured from **c** and **a** respectively. The experimental values are along the directions indicated.

Model		g-tensor		
V_{Li} (a) O_I		2.0373	2.0288	2.0078
	θ	89	89	2
	ϕ	-34	56	
V_{Li} (b) O_{II}		2.0302	2.0119	2.0356
	θ	69	71	29
	ϕ	17	-65	64
V_{Li} (b) O_I		2.0403	2.0125	2.0301
	θ	90	73	17
	ϕ	-27	64	62
Expt.[13]		2.0088	2.0205	2.0366
		a	b	c
V_{Ga} (a) O_{II}		2.0220	2.0514	2.0078
	θ	84	88	6
	ϕ	-35	55	
V_{Ga} (b) O_I		2.0081	2.0228	2.0449
	θ	88	85	5
	ϕ	-16	74	
Expt.[13]		2.0155	2.0551	2.0032
		a	b	c

still be either O_I or O_{II}. Our results for all the cases considered are summarized in Fig. 1, the g-tensors are summarized in Table I and the SHF tensors are given in Table II.

For the V_{Ga} we examine both the apical and basal plane O_I as atom for the hole to localize on. As shown in Fig. 1 (lower-left) and in Table I we find the g-tensor for the apical O_{II} has its smallest g along the direction of the spin density, which is along **c**. This agrees with experiment.[13] The largest principal axis (principal axis corresponding to largest Δg) in the **ab**-plane is 55° from **a** so closer to **b** which also agrees with experiment. In fact it is close to the O_{II}-Ga direction. The Δg themselves are in agreement to about ± 0.005. For the basal plane O_I location of the spin, (Fig. 1 lower-right) on the other hand the main principal axis of the g tensor is along **c**. In both cases it is perpendicular to the spin direction of the spin density p-orbital which corresponds to the lowest Δg direction. The SHF interaction (given in Table II) in both cases is with one Ga atom because obviously the O on which the spin has localized has already lost one of its Ga neighbors and each O is coordinated with two Ga and two Li. It is called a SHF interaction because the nucleus with which the electron spin is interacting is not on the atom on which the spin is localized but one of its neighbors. The hyperfine tensor A is nearly isotropic with a value of about 33 G in excellent agreement with the experimental values of about 37 G. Our values are about 10% underestimated. In agreement with experiment we find a slightly larger A component in the **c** direction for the apical O. The hyperfine with O is not observed because O is more than 99.9 % isotopically in a form which does not carry a nuclear spin. The hyperfine principal axes are indicated by the small arrows in Fig. 1 and are seen to be close to the bond directions rather than the overall crystal axes. While the Li SHF interactions were not observed we give the calculated values for them in Table II in case future measurements would be able to measure them. The reason why they are much smaller is that the atomic wavefunction on the Li nuclear sites are much smaller than on the Ga.

The V_{Li} with spin localized on an apical O_I has its main Δg-tensor component at about 30° from the **a**-axis and its lowest component and spin density along **c** as can be seen in Fig. 1 (upper left). This, however does not agree with the experimental data of Lenyk *et al.*[13] who find the Δg tensor to be oriented with its highest value along **c**. We have calculated two distinct configurations with spin localized on a basal plane O_I and O_{II} (See Table I). For the O_{II} case we find that the lowest Δg is coincident with the direction of the spin density and is close to the bond direction from V_{Li} to the O_{II}. So, it is tilted away from the **ab**-plane by about 30° and close to 60° degrees from the **a**-axis. Note, however, that there is an equivalent O_{II} along the **a** axis in the **ab**-plane projection, which is simply 120° rotated from the one reported in Table I. The highest g-component principal axis has to be perpendicular to this and indeed we find it to be tilted about 30° from the **c**-axis. This model agrees closely with the one proposed by Lenyk *et al.*[13] with the sole difference that they consider the equivalent O_{II} in the **a**-direction. As the authors mention, the occurrence of several distinct magnetic orientations prevents them from carrying out a full study of the angular variation with magnetic field because of the overlap of different signals. As for the O_I basal plane, neighbor, in that case the lowest g-component is along the corresponding $V_{Li}-O_I$ direction at about 60° from the **a** axis. However, the largest g is then found at about $-30°$ from **a** and tilted toward the basal plane. This does not agree with the center identified by Lenyk *et al.*[13]

The SHF splitting in V_{Li} with spin localized on O_{II} is with two nonequivalent Ga. Although all Ga atoms are equivalent in the perfect crystal, the local symmetry is broken. The Ga with smaller SHF A tensor lies closer to the V_{Li} than the other which lies opposite to it from the O_{II} on which the spin is localized. In the experiment, also a slightly nonequivalent Ga-SHF splitting was reported but they estimated the A's to differ by only 4% whereas we find them to differ by about 20%. In agreement with experiment the A tensors are found to be nearly isotropic. The experimental value for the SHF splitting is closer to the larger of the two calculated A and is in good agreement with experiment. For the apical O_I case, one would expect the two Ga neighbors to be equivalent but in the calculation, they are still found to differ by about 20%, which may result from the symmetry breaking in the relaxation calculation.

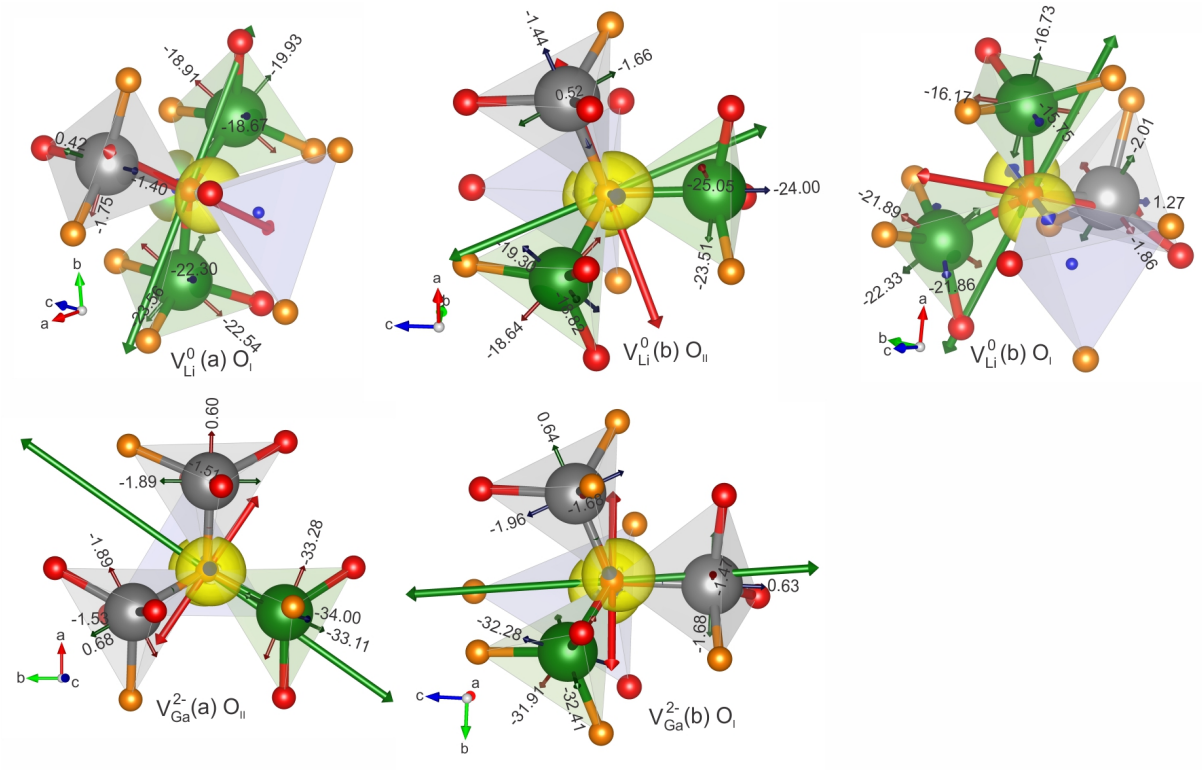

FIG. 1. EPR models for various localizations of the spin density near V_{Li} (top) and V_{Ga} (bottom) obtained in GGA+U. The spin density is shown as the yellow isosurfaces, the g-tensor (calculated using GIPAW) is shown as large green, red, and blue double arrows with size proportional to Δg and direction indicating the principal axes, green spheres indicate Ga with strong hyperfine interaction, silver spheres indicate Li, red spheres O_I, and orange spheres O_{II}. The small arrows on each atom indicate the principal axes and sizes of the hyperfine tensor $\mathbf{A}$. The light blue tetrahedron and blue dots indicate the vacancy site.

TABLE II. Calculated A-tensors of Li and Ga vacancies (in Gauss) calculated using the GIPAW code within GGA+U. The principal values and principal axes directions are given in spherical angles θ and ϕ (θ is measured from $\mathbf{c}$ and ϕ from $\mathbf{a}$). The experimental results give the values along specific crystallographic directions as indicated and the two Ga neighbors are not distinguished because in principle equivalent. The Li hyperfine A were not yet measured.

Model		Ga1			Ga2			Li1			Li2		
V_{Li} (a) O_I		-19.93	-18.91	-18.67	-23.56	-22.54	-22.30	0.42	-1.75	-1.40			
	θ	80	61	31	80	61	31	81	90	9			
	ϕ	-51	33	57	-51	33	57	62	-28	60			
V_{Li} (b) O_{II}		-18.82	-18.64	-19.30	-23.51	-25.05	-24.00	-1.66	0.52	-1.44			
	θ	80	88	10	68	48	51	34	68	66			
	ϕ	-34	56	-48	-85	27	-14	62	9	-70			
V_{Li} (b) O_I		-16.17	-16.73	-15.75	-21.89	-21.86	-22.33	1.27	-2.00	-1.86			
	θ	34	88	57	33	58	83	12	89	78			
	ϕ	81	-12	77	34	49	-46	65	-31	59			
Expt.[13]		24.30	25.00	25.30	24.30	25.00	25.30						
		a	b	c	a	b	c						
V_{Ga} (a) O_{II}		-33.11	-33.28	-34.00				-1.89	0.60	-1.51	0.68	-1.89	-1.53
	θ	67	90	23				89	80	10	80	88	10
	ϕ	67	-23	68				90	0		-62	28	
V_{Ga} (b) O_I		-32.41	-31.91	-32.28				-1.68	-1.47	0.63	0.64	-1.68	-1.96
	θ	72	55	41				89	80	10	66	72	31
	ϕ	56	-47	-11				88	-2		-70	11	68
Expt.[13]		37.50	37.40	35.90									
		a	b	c									

Having identified the apical O as the location of the spin density near a V_{Ga} and the basal plane O near a V_{Li} that best agree with experiment, we may ask whether these indeed correspond to the lowest total energy. It turns out, however, that the energy differences between these different localization sites is quite small. We find that the V_{Ga} has 0.01 eV higher energy per 128 atom cell in the apical than the basal plane site within PBE0,[28] (this is a hybrid functional with 25 % exact and unscreened exchange) so opposite to the experimental identification. For the V_{Li} it is the apical oxygen that was found to have the lower energy by 0.002 eV. In the HSE functional, the apical site was found upon automatic relaxation for both cases. Clearly these energy differences are too small to trust within DFT or at least this is very challenging for any level of theory. Therefore we expect that several of these slightly different forms of the vacancy EPR centers with spin localized on different O-neighbors could be present in experiment but the overlap of these signals would make it difficult to disentangle them. The apical O_{II} for V_{Ga} and basal-plane O_{II} for V_{Li} agree best with the experimental observations but in the V_{Li} case, there would still be two differently oriented forms of this same defect.

Finally, we address the question under what conditions these EPR signals were observed. A hybrid functional study of the native defects in $LiGaO_2$ was recently presented by some of us.[27] From that study, we find that the V^0_{Li} has lower energy than the V^0_{Ga} for all chemical conditions as restricted by the formation of competing binary compounds and under Li-poor conditions can be lower than 1 eV. The V_{Ga} usually has quite high energy (10 eV for Ga-rich conditions and $\sim$4.5 eV under the most Ga-poor, Li-rich conditions allowed) and is not expected to occur in significant concentration in equilibrium. In contrast, the V^-_{Li} is found to be the major acceptor compensating the $\mathrm{Ga}^{2+}_{\mathrm{Li}}$ antisite and is thus expected to be present in the as grown samples. The V_{Li} occurs in 0 and -1 charge states, the former of which contains an unpaired spin and is hence EPR active. Its $0/-$ transition level lies at 1.03 eV above the valence band maximum (VBM). The Ga-vacancy accommodates four charge states, 0, -1,-2, -3. The Fermi level is pinned by the compensation of $\mathrm{Ga}^{2+}_{\mathrm{Li}}$ antisites with V^-_{Li} and to some extent by $\mathrm{Li}^{2-}_{\mathrm{Ga}}$ in Li-rich conditions. In both cases, the Fermi level lies deep below the conduction band between 2.7-3.8 eV above the VBM straddling the $2-/3-$ transition level of the V_{Ga}, which occurs at 3.3 eV. The V_{Ga}, once it is formed, may thus be expected to be found in the EPR active $q = -2$ charge state in particular for the deeper Fermi level position, which occurs for more realistic assumptions of the O-chemical potential.

The above findings agree with the observations of Lenyk *et al.*[13] that high-energy particle irradiation is required to create the V_{Ga}. However, the fact that they do not require to be optically activated once formed indicates a $2-$ charge state after irradiation. On the other hand the Li-vacancies were found to be present already in as-grown material. This however does not imply the material was Li-poor. Even under both Li and Ga rich conditions, the V_{Li} has an energy of formation significantly lower than that of Ga. However, the fact that its $0/-$ level lies only 1.02 eV above the VBM clearly explains why the Li must be activated optically by removing an electron from it. In the experiments by Lenyk *et al.*[13] this is achieved by application X-rays.

In conclusion, our first-principles calculations confirm the experimental assignment of the EPR centers of V_{Ga} and V_{Li} by Lenyk *et al.*[13] For the V_{Ga} the spin is localized on an apical O_{II} and for the V_{Li} it is on a basal plane O_{II}. The orientations of the principal axes of the g-tensor and A-tensors are found to be closely related to the bond directions and in the V_{Li} case two different orientations of the defect center with respect to the crystal axis should exist with overlapping spectra. The EPR parameters for alternative localizations of the spin on different O-neighbors were also calculated and found to be different. As these different forms of localization of the spin have total energies close to each other they might possibly occur in the real systems and we hope that providing the associated parameters here could assist in disentangling these different EPR centers. For the cases observed so far, our g-tensor and SHF interaction parameters are in good agreement with experiment. Our calculations also explain why the V_{Ga} defects require high energy radiation to be formed but no further optical activation while the opposite is the case for the V_{Li}.

Acknowledgements: The work at CWRU was supported by the U.S. National Science Foundation under grant No. 1755479. This work used the Extreme Science and Engineering Discovery Environment (XSEDE) Stampede2 at the UT Austin through allocation TG-DMR180118.

* Corresponding author dmitry.skachkov@case.edu, Current address: Department of Physics, University of Florida, Gainesville, Florida 32611

[1] M. Marezio, Acta Crystallographica **18**, 481 (1965).
[2] T. Ishii, Y. Tazoh, and S. Miyazawa, J. Crystal Growth **186**, 409 (1998).
[3] J. T. Wolan and G. B. Hoflund, J. Vac. Sci. Tech. A **16**, 3414 (1998).
[4] N. W. Johnson, J. A. McLeod, and A. Moewes, Journal of Physics: Condensed Matter **23**, 445501 (2011).
[5] C. Chen, C.-A. Li, S.-H. Yu, and M. M. Chou, Journal of Crystal Growth **402**, 325 (2014).
[6] I. Ohkubo, C. Hirose, K. Tamura, J. Nishii, H. Saito, H. Koinuma, P. Ahemt, T. Chikyow, T. Ishii, S. Miyazawa, Y. Segawa, T. Fukumura, and M. Kawasaki, Journal of Applied Physics **92**, 5587 (2002).

[7] T. Omata, K. Tanaka, A. Tazuke, K. Nose, and S. Otsuka-Yao-Matsuo, J. Appl. Phys. **103**, 083706 (2008).
[8] T. Omata, M. Kita, K. Nose, K. Tachibana, and S. Otsuka-Yao-Matsuo, Jpn. J. Appl. Phys. **50**, 031102 (2011).
[9] S. Nanamatsu, K. Doi, and M. Takahashi, Japanese Journal of Applied Physics **11**, 816 (1972).
[10] S. N. Gupta, J. F. Vetelino, V. B. Jipson, and J. C. Field, Journal of Applied Physics **47**, 858 (1976).
[11] A. Boonchun and W. R. L. Lambrecht, Phys. Rev. B **81**, 235214 (2010).
[12] A. Boonchun and W. R. L. Lambrecht, in *Oxide-based Materials and Devices II*, Proceedings of SPIE, Vol. 7940, edited by F. H. Terani, D. C. Look, and D. J. Rogers, International Society for Optics and Photonics (SPIE, 2011) pp. 129–134.
[13] C. A. Lenyk, M. S. Holston, B. E. Kananen, L. E. Halliburton, and N. C. Giles, Journal of Applied Physics **124**, 135702 (2018).
[14] C. J. Pickard and F. Mauri, Phys. Rev. B **63**, 245101 (2001).
[15] C. J. Pickard and F. Mauri, Phys. Rev. Lett. **88**, 086403 (2002).
[16] U. Gerstmann, M. Rohrmller, F. Mauri, and W. Schmidt, Physica Status Solidi (c) **7**, 157 (2010).
[17] D. Ceresoli, U. Gerstmann, A. P. Seitsonen, and F. Mauri, Phys. Rev. B **81**, 060409 (2010).
[18] `http://qe-forge.org/gf/project/qe-gipaw/`.
[19] P. Giannozzi, S. Baroni, N. Bonini, M. Calandra, R. Car, C. Cavazzoni, D. Ceresoli, G. L. Chiarotti, M. Cococcioni, I. Dabo, A. Dal Corso, S. de Gironcoli, S. Fabris, G. Fratesi, R. Gebauer, U. Gerstmann, C. Gougoussis, A. Kokalj, M. Lazzeri, L. Martin-Samos, N. Marzari, F. Mauri, R. Mazzarello, S. Paolini, A. Pasquarello, L. Paulatto, C. Sbraccia, S. Scandolo, G. Sclauzero, A. P. Seitsonen, A. Smogunov, P. Umari, and R. M. Wentzcovitch, Journal of Physics: Condensed Matter **21**, 395502 (19pp) (2009).
[20] V. I. Anisimov, J. Zaanen, and O. K. Andersen, Phys. Rev. B **44**, 943 (1991).
[21] V. I. Anisimov, I. V. Solovyev, M. A. Korotin, M. T. Czyżyk, and G. A. Sawatzky, Phys. Rev. B **48**, 16929 (1993).
[22] A. I. Liechtenstein, V. I. Anisimov, and J. Zaanen, Phys. Rev. B **52**, R5467 (1995).
[23] J. Heyd, G. E. Scuseria, and M. Ernzerhof, J. Chem. Phys. **118**, 8207 (2003).
[24] J. Heyd, G. E. Scuseria, and M. Ernzerhof, J. Chem. Phys. **124**, 219906 (2006).
[25] D. Skachkov, W. R. L. Lambrecht, H. J. von Bardeleben, U. Gerstmann, Q. D. Ho, and P. Dek, Journal of Applied Physics **125**, 185701 (2019).
[26] D. Skachkov and W. R. L. Lambrecht, Applied Physics Letters **114**, 202102 (2019).
[27] A. Boonchun, K. Dabsamut, and W. R. L. Lambrecht, J. Appl. Phys. **126**, 155703 (2019).
[28] J. P. Perdew, M. Ernzerhof, and K. Burke, J. Chem. Phys. **105**, 9982 (1996).